

# Synthesizing of Functionally Graded Surface Composites by Laser Powder Deposition Process for Slurry Erosion Applications

Ehsan Foroozmehr<sup>1</sup>, Rouzbeh Sarrafi<sup>1</sup>, Syed Hamid<sup>2</sup>, Radovan Kovacevic<sup>1</sup>

<sup>1</sup>Center for Laser Aided Manufacturing, (CLAM), Southern Methodist University, Dallas, Texas

<sup>2</sup>Halliburton Energy Services, Carrollton, Texas

Reviewed, accepted September 15, 2009

## Abstract

Metal-ceramic composites are used extensively in surface modification. Laser cladding, as one of the surface treatment techniques, shows a promising method to deposit functionally graded layers of metal-ceramic composite. In this study, AISI 4140 and nickel as the matrix and tungsten carbide (WC), titanium carbide (TiC), and nano-WC as the ceramic parts are used in four different combinations for deposit on AISI 4140 substrates. The volume percentage of the ceramics is increased from the bottom to the top. The microstructure and micro-hardness of the samples and residual stress of the top surface of the samples are studied and compared.

## 1. Introduction

The laser powder deposition process is widely used to improve the surface quality of components in harsh working conditions. Depending on the application, different coating materials can be used. Metal matrix composites (MMC) are receiving much attention because of their excellent combination of ductility and toughness of the metallic matrix with high hardness and strength of the ceramic particles reinforced in the matrix [1]. Different ceramic materials such as TiC and WC are used in MMC coatings, such as Ni-based [2-4], Co-based [5, 6], and steel based composites [1, 7-10].

TiC, due to its high hardness, melting point, thermodynamic stability, and availability is one of the common ceramic materials used in MMC coatings. Jiang and Kovacevic [1] reported a promising improvement in slurry erosion resistance of steel substrates in laser deposition of TiC/H13 composite. WC is another popular ceramic that is used in micro and nano scales in MMC applications. Yarrapareddy and Kovacevic [3] reported the advantage of using nano-sized combined with micro-sized WC particles in the laser cladding of Ni-WC composite. Laser cladding of WC in a Co-based matrix with a composition of over 10-20% shows a high susceptibility of cracking due to formation of some brittle intermetallics [5, 6].

Slurry erosion introduces a loading condition that requires hard surface of the component under the load as well as a minimum of ductility to overcome the dynamic loading condition and fatigue. Sharp change of the material properties from a soft substrate to a hard coating causes stress concentration. Functionally graded material (FGM) has been shown a proper solution to overcome the mentioned problems to some extent [8]. By gradually changing the ceramic content of

the coating from the bottom to the top, the sharp change of the material properties is reduced. In addition, the bottom layers have higher ductility that increases the fatigue life of the component.

In this paper, four material systems in a functionally graded form are deposited on substrates of AISI 4140: 4140-WC, 4140-TiC, Ni-WC, and Ni-WC-nano WC to enhance the slurry erosion resistance of the surface. The powder mesh size for 4140, Ni, TiC, and WC powder is -140/+325. The optical and SEM micrographs of the cross-section of the coupons as well as the micro-hardness of the matrix are demonstrated as the primary results of this study. The results final slurry erosion resistance of the material systems will be published accordingly.

## 2. Experimental setup

In order to study the microstructure of different MMCs, a series of experiments are performed. The MMC powder, for each composition, is mixed using a ball-mill mixer with ceramic balls prior to the experiments. The micro-sized powders are mixed for about an hour while the mixture containing the nano-sized powder is mixed for over 20 hours to increase the homogeneity. The experimental setup consists of a 1-kW continuous wave Nd:YAG laser system assisted with a deposition head, a 5-axis CNC vertical machining center, and a powder feeding system with argon as carrying gas. The process parameters of the experiments are listed in Table 1.

**Table 1. Process parameters**

Laser power (W)	340-370
Scanning speed (mm/sec)	8-10
Powder feed rate (g/min)	2.5-3
Beads overlap (%)	35

With the mentioned process parameters, the average bead width and height are 0.5 and 0.25 mm, respectively. Each composition is deposited in three layers on the substrates of 75 x 25 x 6 mm with the volume percentage of the ceramic phase increasing from the bottom to the top layer as shown in Table 2.

**Table 2. Composition of each layer of the FGM parts**

<b>4140 – WC</b> <b>4140 – TiC</b> <b>Ni – WC</b>	1 <sup>st</sup> layer (bottom)	80 – 20 %
	2 <sup>nd</sup> layer (middle)	50 – 50 %
	3 <sup>rd</sup> layer (top)	20 – 80 %
<b>Ni – WC – nano WC</b>	1 <sup>st</sup> layer	80 – 15 – 5 %
	2 <sup>nd</sup> layer	50 – 45 – 5 %
	3 <sup>rd</sup> layer	20 – 75 – 5 %

After performing the experiments, the coupons are cross cut using a waterjet cutting system. The samples are mounted, ground, and polished according to standard metallography methods. The microstructure of the coupons is studied using an optical microscope and scanning electron microscope (SEM). The hardness of the matrix is studied using a micro-hardness testing machine with 200-g load and a 15 sec dwell time.

### 3. Results and discussions

The microstructure of the deposits is studied in this section.

#### 3.1 4140 – WC composite

An overview of the 4140 – WC FGM deposit is shown in Fig. 1. WC particles are seen in different sizes (from 10 to 100  $\mu\text{m}$ ). The spatial distribution of WC particles in each layer is almost uniform. However, the number of long cracks, elongated mostly in the thickness direction and passing through the matrix and the WC particles, is observed in the deposit. Fig. 2 shows a typical crack observed in the deposit. These cracks that might be generated during the cross-sectioning process imply the brittle nature of the coating, and therefore, not suitable for applications such as slurry erosion in which ductility and hardness are both critical [3]. The micro-hardness measurements of the composite matrix in the thickness direction (Fig. 3) also show signs of embrittlement. As can be seen, a very high value of hardness, especially at the top layers where the volume percentage of the WC is maximum, is observed. There is a strong affinity between the steel matrix and the carbon in WC particles as reported in the machining literature [11]. This strong affinity causes the migration of carbon to the steel matrix and the consequent embrittlement. The embrittlement of the matrix along with the relatively high stresses developed during laser cladding could cause the cracking of the 4140-WC composite. Due to the severe cracking, this composition does not seem to be suitable for erosion applications that demand a high-strength material with a proper level of ductility and toughness.

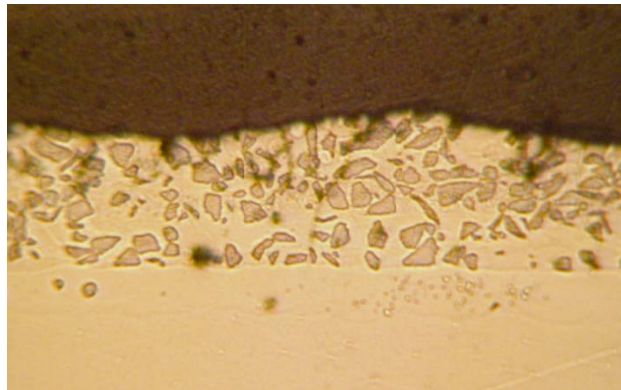


Fig. 1. 4140-WC deposit

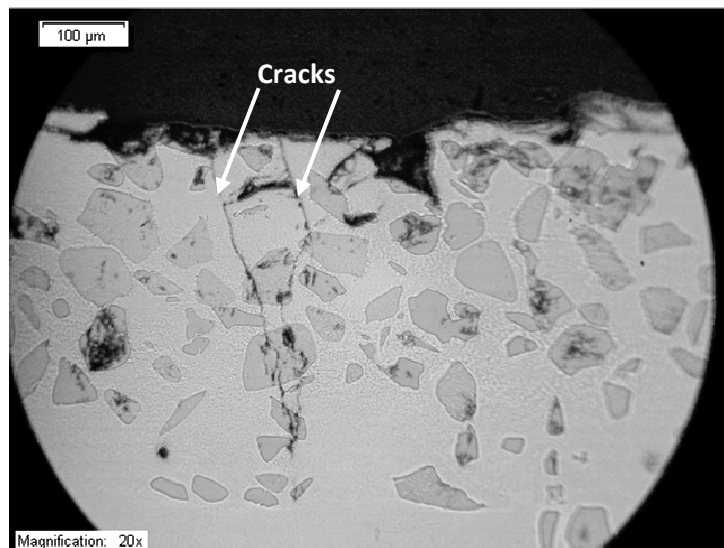


Fig. 2. A typical crack observed in the direction of thickness

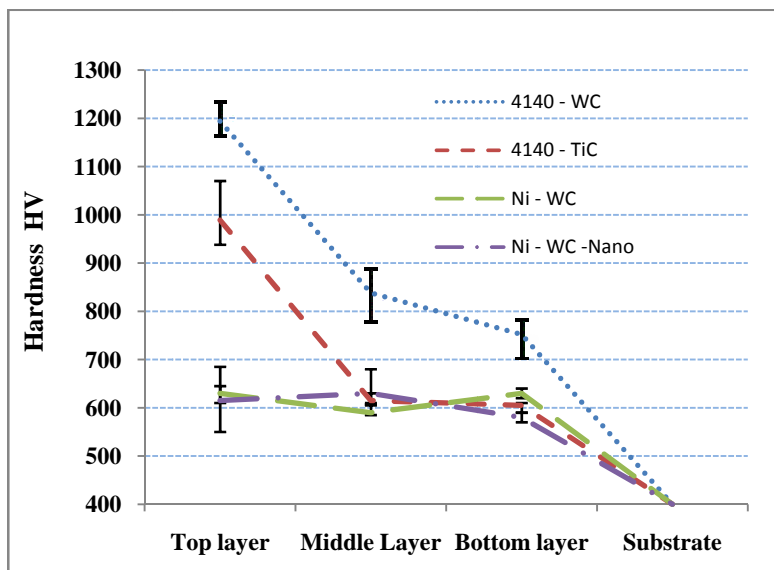


Fig. 3. Micro-hardness of the matrix of surface composites

### 3.2 4140 – TiC composite

4140-TiC FGM composite is sound, and no crack or discontinuity is observed in the deposit. As shown in Fig. 4, the concentration of TiC particles varies along the thickness of the coating as the percentage of the TiC in the composite increases. A closer view of the cross-section reveals the presence of precipitates of TiC within the matrix. This precipitation, however, varies from the bottom to the top of the coating. Fig. 5a to 5c show backscattered (BS) SEM micrographs of the first, second, and third layers, respectively. As shown in Fig. 5a, beside the large TiC particles, there are a number of tiny TiC precipitates in the matrix. A higher magnification of these flower-shaped precipitates is shown in the same figure. By increasing the volume percentage of TiC in the composite, the shape and concentration of the precipitates are changed. Fig. 5b shows the precipitates that have a dendritic shape. By increasing the TiC percentage in the top layer (Fig. 5c), a more dendritic shape of the precipitates can be observed. The effect of the presence of the precipitated TiC particles in the matrix can be directly seen in the micro-hardness test shown in Fig. 3. As can be expected, a higher hardness is obtained in the third layer.

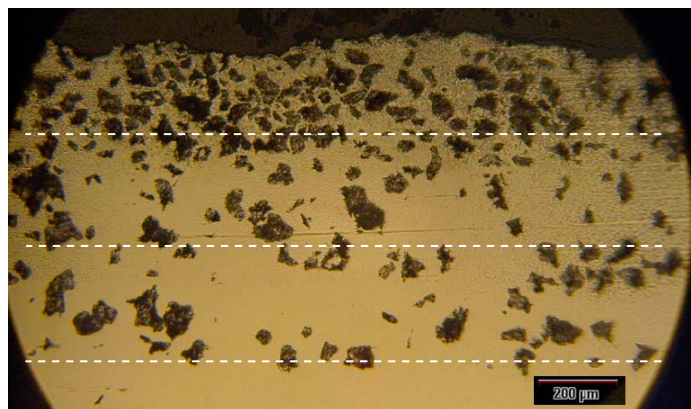


Fig. 4. 4140-TiC FGM surface composite

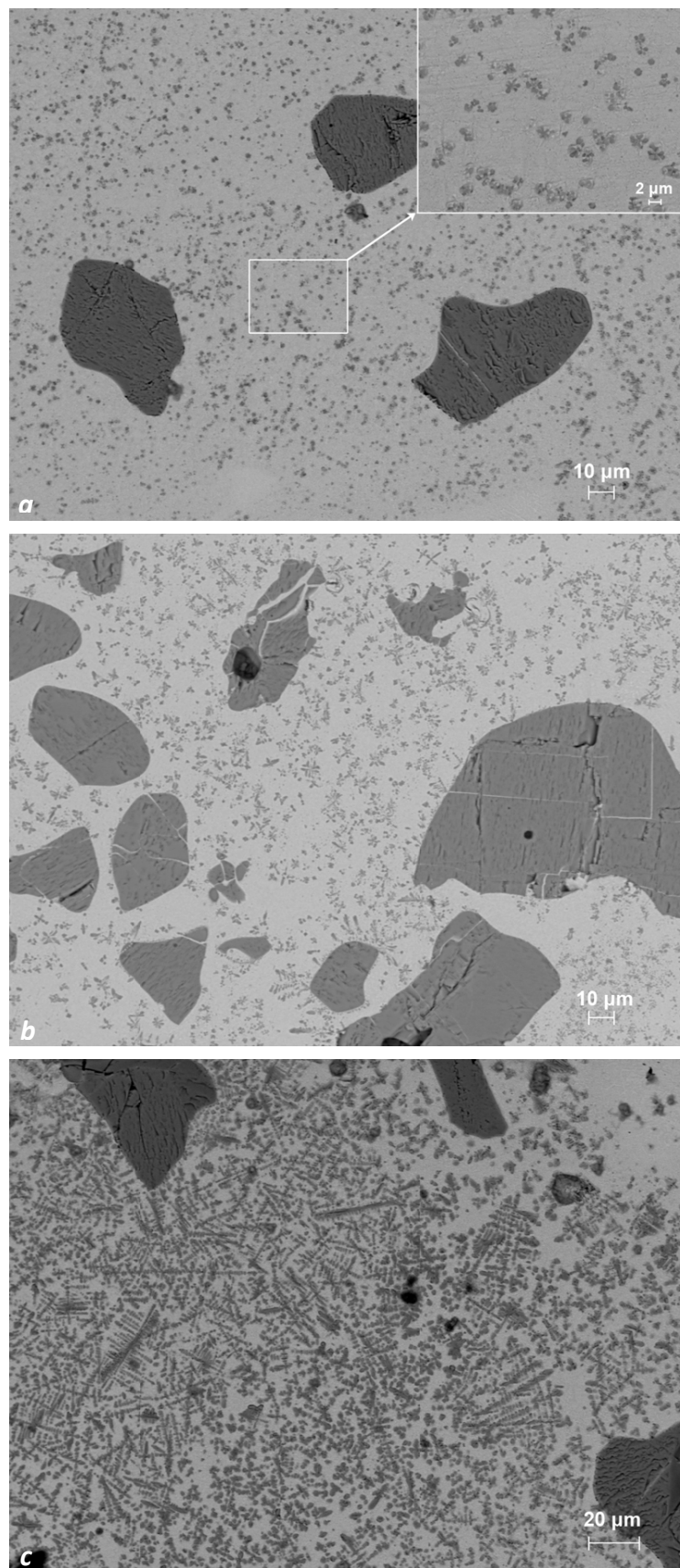


Fig. 5. Fine TiC precipitates scattered between the large TiC particles: (a) first layer, (b) second layer, (c) third layer

### 3.3 Ni – WC composite

The Ni-WC FGM composite is sound, and no crack or discontinuity is observed in the deposit. The distribution of WC particles in the nickel matrix varies along the thickness of the coating by increasing the percentage of WC in the matrix, as shown in Fig. 6. In between the large particles of WC, some small particles of WC can be recognized that are believed to be broken pieces of large WC particles that occurred during the mixing of the powders. No sign of significant melting of WC particles is observed. Since there is no dissolution and precipitation of WC particles in the nickel matrix, the micro-hardness of the Ni matrix does not vary from the bottom layer to the top one, as shown in Fig. 3.

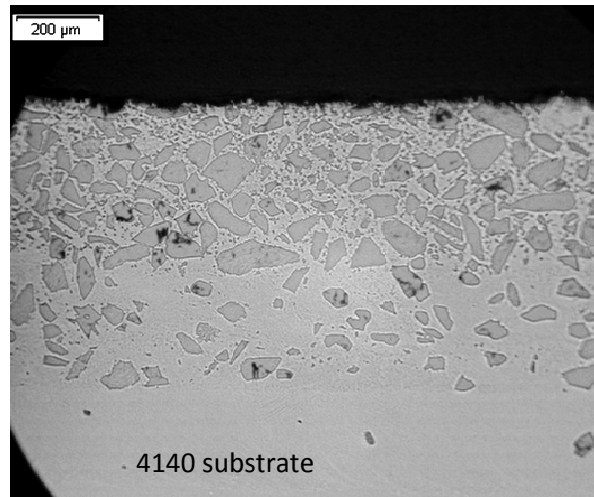


Fig. 6. Ni-WC FGM surface composite.

### 3.4 Ni – WC + Nano WC composite

Adding nano-particles to the Ni-WC composite shows some noticeable change in the microstructure of the coating. Because of the longer mixing time necessary for reaching good homogeneity of the nano particles, the amount of broken pieces of WC particles are increased. In addition, in between the large and broken pieces of WC, a number of clusters of nano-WC particles can be found. Fig. 7 shows all three types of particles in the matrix of Ni. The micro-hardness test of this composite shows a relatively constant hardness for the matrix (shown in Fig. 3). It should be noted again that the reported values are the hardness of the matrix alone. As the distribution of the nano-WC particles is not completely homogeneous, it is feasible to find places on the matrix to measure just the hardness of the matrix. A similar study is performed by Yarrapareddy and Kovacevic [3] where it is shown that the presence of nano-WC particles in the matrix improves the strength of the coating in the slurry erosion application.

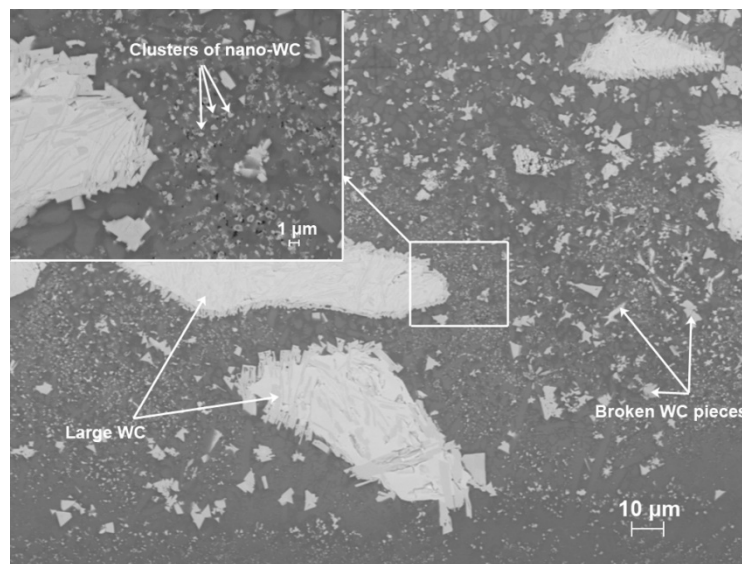


Fig. 7. Microstructure of Ni-WC-nano-WC composite

#### 4. Conclusions

Four different graded surface composites are deposited on a 4140 steel substrate. The microstructure and matrix microhardness are studied. The following conclusions can be drawn:

1. The 4140- WC composite suffers from severe cracking, which is a consequence of the dissolution of WC in the steel substrate.
2. The produced 4140-TiC surface composite is sound and crack-free. The TiC particles are partially dissolved and precipitate as fine dendrites throughout the matrix between the large particles of TiC. The precipitates' structure varies from the bottom to the top layer by changing the percentage of TiC in the matrix.
3. The deposited Ni-WC composites are sound and crack free. No significant dissolution and precipitation of WC in the Ni matrix is observed.
4. In the deposition of Ni-WC-nano-WC composite, nano-WC particles are successfully dispersed throughout the Ni matrix and among the large WC particles.

#### 5. Acknowledgment

This work was partially funded by NSF Grant No. EEC-0541952.

#### 6. References

- [1] W.H. Jiang, R. Kovacevic, "Laser deposited TiC/H13 tool steel composite coatings and their erosion resistance," *Journal of Material Processing Technology*, Vol. 186, pp. 331-338, 2007.
- [2] Q. Li, T.C. Lei, W.Z. Chen, "Microstructural characterization of laser-clad TiC<sub>p</sub>-reinforced Ni-Cr-B-Si-C composite coatings on steel," *Journal of Surface and Coating Technology*, Vol. 114, No. 2-3, pp. 278-284, 1999.

- [3] E. Yarrapareddy, R. Kovacevic, "Synthesis and characterization of laser-based direct metal deposited nano-particles reinforced surface coatings for industrial slurry erosion applications," *Journal of Surface and Coating Technology*, Vol. 202, pp. 1951-1965, 2008.
- [4] M.J. Tobar, J.M. Amado, J.C. Alvarez, J. Lamas, A. Yanez, "Laser cladding of tungsten carbide hardfacing alloys on steels used in mining industry," *Laser Material Processing Conference, ICALEO2008 Congress Proceedings*, pp. 734-738, 2008.
- [5] M. Zhong, K. Yao, W. Liu, "High-power laser cladding Stellite 6+WC with various volume rates," *Journal of Laser Applications*, Vol. 13, No. 6, pp. 247-251, 2001.
- [6] G.J. Xu, M. Kutsuna, "Cladding with Stellite 6+WC using a YAG laser robot system," *Journal of Surface Engineering*, Vol. 22, No. 5, pp. 345-352, 2006.
- [7] H. Mei, J. Ouyang, D. Hu, R. Kovacevic, "Rapid fabrication of functionally gradient material parts by laser beam," *Laser Material Processing Conference, ICALEO2003 Congress Proceedings*. 2003.
- [8] A. Yakovlev, P. Bertrand, I. Smurov, "Development of 3D functionally graded models by laser-assisted coaxial powder injection," *Laser-Assisted Micro- and Nanotechnologies 2003. Edited by Veiko, Vadim P. Proceedings of the SPIE*, Vol. 5399, pp. 220-227, 2004.
- [9] S. Ariely, J. Shen, M. Bamberger, F. Dausiger, H. Hugel, M. Geller, "Laser surface alloying of steel with TiC," *Journal of Surface and Coating Technology*, Vol. 45, No. 1-3, pp. 403-408, 1991.
- [10] C. Tassin, F. Laroudie, M. Pons, L. Lelait, "Carbide-reinforced coatings on AISI 316 L stainless steel by laser surface alloying," *Journal of Surface and Coating Technology*, Vol. 77, No. 1-3, pp. 450-455, 1995.
- [11] M. P. Groover, "Fundamentals of modern manufacturing," *John Wiley and Sons*, pp. 554, 2007.